The Journal of Immunology

MicroRNA-15b Modulates Japanese Encephalitis Virus–Mediated Inflammation via Targeting RNF125

Bibo Zhu, Jing Ye, Yanru Nie, Usama Ashraf, Ali Zohaib, Xiaodong Duan, Zhen F. Fu, Yunfeng Song, Huanchun Chen and Shengbo Cao

J Immunol 2015; 195:2251-2262; Prepublished online 22 July 2015;
doi: 10.4049/jimmunol.1500370
http://www.jimmunol.org/content/195/5/2251

The Journal of Immunology is published twice each month by
The American Association of Immunologists, Inc.,
1451 Rockville Pike, Suite 650, Rockville, MD 20852

Print ISSN: 0022-1767 Online ISSN: 1550-6606.

MicroRNA-15b Modulates Japanese Encephalitis Virus–Mediated Inflammation via Targeting RNF125

Bibo Zhu,*,†,‡ Jing Ye,*,†,‡ Yanru Nie,*,†,‡ Usama Ashraf,*,† Ali Zohaib,*,† Xiaodong Duan,*,†,‡ Zhen F. Fu,*,†,‡,§ Yunfeng Song,*,†,‡ Huanchun Chen,*,†,‡ and Shengbo Cao*,†,‡

Japanese encephalitis virus (JEV) can target CNS and cause neuroinflammation that is characterized by profound neuronal damage and concomitant microgliosis/astrogliosis. Although microRNAs (miRNAs) have emerged as a major regulatory network with profound effects on inflammatory response, it is less clear how they regulate JEV-induced inflammation. In this study, we found that miR-15b is involved in modulating the JEV-induced inflammatory response. The data demonstrate that miR-15b is upregulated during JEV infection of glial cells and mouse brains. In vitro overexpression of miR-15b enhances the JEV-induced inflammatory response, whereas inhibition of miR-15b decreases it. Mechanistically, ring finger protein 125 (RNF125), a negative regulator of RIG-I signaling, is identified as a direct target of miR-15b in the context of JEV infection. Furthermore, inhibition of RNF125 by miR-15b results in an elevation in RIG-I levels, which, in turn, leads to a higher production of proinflammatory cytokines and type I IFN. In vivo knockdown of virus-induced miR-15b by antagomir-15b restores the expression of RNF125, reduces the production of inflammatory cytokines, attenuates glial activation and neuronal damage, decreases viral burden in the brain, and improves survival in the mouse model. Taken together, our results indicate that miR-15b modulates the inflammatory response during JEV infection by negative regulation of RNF125 expression. Therefore, miR-15b targeting may constitute an interesting and promising approach to control viral-induced neuroinflammation. ***The Journal of Immunology*****, 2015, 195: 2251–2262.**

The inflammatory response constitutes an important immune defense against host invasion by microbial pathogens (1). It is a protective process by the body to ensure clearance of detrimental stimuli. However, an excessive inflammatory response to overwhelm pathogens can be fatal (1). Japanese encephalitis virus (JEV) is an ssRNA virus belonging to the genus *Flavivirus* of the Flaviviridae family (2). JEV-induced encephalitis is the most prevalent viral encephalitis in the Asia-Pacific region of the world (3). Approximately, 35,000–50,000 cases of Japanese encephalitis are reported annually in Asia, with 10,000 deaths; nearly half of the survivors suffer from permanent neuropsychiatric sequelae (4, 5). Japanese encephalitis is characterized by profound neuronal damage along with substantial activation of glial cells, including microglias and astrocytes (6). During infection, JEV targets the CNS and generates a rapid inflammatory response, resulting in increased levels of cytokines, such as TNF-α, IL-6, IL-1β, MCP-1, and RANTES, in the cerebrospinal fluid. The increased levels of inflammatory mediators appear to play a protective role or to initiate an irreversible immune response leading to neuronal death (7). Microglias and astrocytes are the resident immune cells in the CNS and represent critical effectors of CNS inflammation (8, 9). It was reported that microglias and astrocytes can be directly infected by JEV and act as a reservoir for the virus (8, 10). The production of various proinflammatory mediators has been implicated in the process of activation of microglias and astrocytes following JEV infection (6, 8, 11). However, the regulation of JEV-induced CNS inflammation is not well documented.

MicroRNAs (miRNAs) are noncoding, tiny (~22 nt) RNAs that play a crucial role in posttranscriptional gene regulation by targeting 3′ untranslated regions (UTRs), which results in translational tuning, repression, or degradation (12). Their regulatory potential is vast: as many as 60% of all mRNAs are predicted to be regulated by miRNAs to some extent (13). The role of miRNAs has been widely studied in the regulation of a broad spectrum of cellular processes, including proliferation and differentiation, cancer, apoptosis, and viral infections (14–17). Recently, these small RNAs also were found to be involved in the TLR and RIG-I signaling pathways of the innate immune system (18). In addition, miR-146a, miR-21, and miR-155 are regarded as regulators of IFN signaling and inflammatory responses at multiple levels (19–21). TLR4-mediated activation of NF-κB induces a negative feedback by upregulating miR-21 and miR-146, which ultimately dampen TLR-induced signaling and cytokine expression (22). In contrast, miR-155 shows anti- and proinflammatory effects by regulating TAB2 and SOCS1, respectively (23, 24). Although these miRNAs are associated with fine-tuned inflammatory responses,

*State Key Laboratory of Agricultural Microbiology, Huazhong Agricultural University, Wuhan, Hubei 430070, People's Republic of China; †Laboratory of Animal Virology, College of Veterinary Medicine, Huazhong Agricultural University, Wuhan, Hubei 430070, People's Republic of China; ‡The Cooperative Innovation Center for Sustainable Pig Production, Huazhong Agricultural University, Wuhan, Hubei 430070, People's Republic of China; and §Department of Pathology, University of Georgia, Athens, GA 30602

Received for publication February 13, 2015. Accepted for publication June 19, 2015.

This work was supported by the National Natural Sciences Foundation of China (Grants 31172325 and 31472221), the Special Fund for Agro-scientific Research in the Public Interest (Grant 201203082), the 948 Project (Grant 2011-G24), Fundamental Research Funds for the Central University (Grant 2013PY051), and the Programme of Introducing Talents of Discipline to Universities (Grant B12005).

Address correspondence and reprint requests to Dr. Shengbo Cao, State Key Laboratory of Agricultural Microbiology, Huazhong Agricultural University, Wuhan, Hubei 430070, People's Republic of China. E-mail address: sbcao@mail.hzau.edu.cn

The online version of this article contains supplemental material.

Abbreviations used in this article: GFAP, glial fibrillary protein; HBV, hepatitis B virus; IBA-1, ionized calcium-binding adapter molecule 1; IHC, immunohistochemical; ISG, IFN-stimulated gene; JEV, Japanese encephalitis virus; miRNA, microRNA; MOI, multiplicity of infection; qRT-PCR, quantitative real-time PCR; RNF125, ring finger protein 125; siRNA, small interfering RNA; UTR, untranslated region; WT, wild-type.

miRNA-mediated regulation of neuroinflammation during viral infection has not been investigated in detail.

miR-15b belongs to the miR-15/16 family, and the miR-15b/16-2 cluster is highly conserved among mammalian species (25). miR-15b is widely expressed and plays diverse roles in different tissues and cell types. This miRNA was found to be highly expressed in hepatocellular carcinoma (26) and other tumors (27), indicating the potential importance of miR-15b in cancers. miR-15b also was shown to play very important roles in the regulation of cell proliferation and apoptosis by targeting cell cycle proteins and Bcl-2 protein (28, 29). In hepatocytes, miR-15b promotes hepatitis B virus (HBV) replication by directly targeting HNF1α, whereas HBV replication represses the expression of miR-15b (30). In addition, miR-15b is involved in the expansion and differentiation of neural progenitor cells through cooperation with TET3 (31). In this study, miR-15b was found to regulate JEV-induced inflammation. It is demonstrated that virus-mediated induction of miR-15b increases RIG-I expression by direct suppression of ring finger protein 125 (RNF125), resulting in the aggravation of JEV-induced production of inflammatory mediators. In vivo treatment of JEV-infected mice with antagomir-15b alleviates overall neuroinflammation and improves survival. To the best of our knowledge, this is the first study to elucidate the role of miR-15b as a regulator of JEV-induced inflammation through the targeting of RNF125.

Materials and Methods

Reagents

Abs against RNF125, GAPDH, RIG-I, NF-κB p65, and Lamin A were purchased from Abclonal Technology (Wuhan, China). Abs against phospho-IRF3 and IRF3 were obtained from Cell Signaling Technology (Beverly, MA). HRP-conjugated anti-mouse/rabbit secondary Abs (Boster, Wuhan, China) were used. Abs against the NS5 protein of JEV were prepared as previously described (32). Hsa–miR-15b mimics (dsRNA oligonucleotides), inhibitors (single-stranded oligonucleotides chemically modified by 2′-Ome), and control oligonucleotides were commercially synthesized by GenePharma (Shanghai, China). Their sequences are as follows: hsa–miR-15b mimics, sense: 5′-UAGCAGCACAUCAUGGUUUACA-3′, antisense: 5′-UAAACCAUGAUGUGCUGCUAUU-3′; mimics control, sense: 5′-UUCUCCGAACGUGUCACGUTT-3′, antisense: 5′-ACGUGACACGUUCGGAGAATT-3′; hsa–miR-15b inhibitors, 5′-UGUAAACCAUGAUGUGCUGCUA-3′; and inhibitors control, 5′-CAGUACUUUUGUGUAGUACAA-3′. Cholesterol-conjugated and chemically modified mmu–miR-15b inhibitors (antagomir-15b) were synthesized by GenePharma. The sequence of antagomir-15b is 5′-U_sG_sUAAACCAUGAUGUGCUG$C_sU_sA_s$-Chol-3′. The subscript "s" represent a phosphorothioate linkage, and "Chol" represents cholesterol linked through a hydroxyprolinol linkage. All nucleotides are 2′-Ome modified.

Constructs and plasmids

The psiCheck-2 dual-luciferase reporter vector (Promega) harboring the 3′ UTR of RNF125, which was inserted into the XhoI and NotI restriction sites 3′ to the end of the *Renilla* gene, was used to check the effect of miR-15b on *Renilla* activity. The 3′ UTR of RNF125 was amplified from HeLa cell genomic DNA with the specific primers (forward: 5′-CCCTCGAGCCTTGGACAAGTCTCGTAA-3′ and reverse: 5′-TTGCGGCCGCTCGTGCCTAACCATGATG-3′). The psiCheck-2 mutant RNF125 3′ UTR construct was generated by introducing a point mutation with overlap-extension PCR (33). The following primers were used for overlap-extension PCR: forward: 5′-ATTTAAGATGGACGTTGAACAAATGGGAGGGAAG-3′ and reverse: 5′-CATTTGTTCAACGTCCATCTTAAATGGTGCAATTC-3′. To construct the RNF125 expression vector, the coding regions were amplified from cDNA derived from HeLa cells by PCR using the primers forward, 5′-CCCTCGAGATGGGCTCCGTGCTGAGCACC-3′ and reverse, 5′-GCTCTAGATTATGTGGTGTTCGAGTGATTCACAT-3′ and cloned into pCDNA4 to yield pCDNA-RNF125. To generate RNF125 expression constructs with wild-type (WT) and mutated 3′ UTRs, the 3′ UTR and mutated 3′ UTR were cloned into pCDNA-RNF125 to yield pCDNA-RNF125-3′ UTR WT and pCDNA-RNF125-3′ UTR mutant. All constructs were verified by sequencing.

RNA interference

Small interfering RNAs (siRNAs) and the control siRNA were purchased from GenePharma. siRNAs were used to knock down human RNF125 (5′-CCGUGUGCCUUGAGGUGUU-3′) (34) and RIG-I (5′-GAGGUGCAGUAUAUUCAGG-3′) (35), as well as mouse RNF125 (5′-CAGUCACACUUUGUUUUAU-3′) and RIG-I (5′-GCCCAUUGAAACCAAGAAA-3′) (36). The nonspecific control siRNA sequence used was 5′-UCCUCCGAACGUGUCACGU-3′. Transfection was performed with Lipofectamine 2000. Cells were transfected with 50 nM each siRNA.

Virus titration

The JEV WT strain P3 used in this study was propagated in suckling mouse brain. The titer of virus was determined by plaque assay on BHK-21 cells, as previously described (37).

Cell culture and treatment

BV-2 cells (mouse microglia cell line), U251 cells (human astrocytoma cell line), and HeLa cells (American Type Culture Collection) were cultured and maintained in DMEM supplemented with 10% heat-inactivated FBS, 100 U/ml penicillin, and 100 μg/ml streptomycin sulfate at 37°C in 5% CO_2. BV-2 cells or U251 cells were plated in six-well plates (6×10^5 cells/well) and grown to 80% confluence. Cells were subsequently transfected with plasmids and/or RNAs using Lipofectamine 2000 (Invitrogen), according to the manufacturer's instructions. After 24 h, the cell medium was removed and the cells were infected with medium or JEV (multiplicity of infection [MOI] of 5) for the indicated times.

miRNA target prediction

Putative miRNA target genes were identified using an miRNA database (http://www.mirbase.org/) and target prediction tools: PicTar (http://pictar.mdc-berlin.de/), TargetScan (http://www.targetscan.org/), RNAhybrid (http://bibiserv.techfak.uni-bielefeld.de/rnahybrid/), and MicroCosm (http://www.ebi.ac.uk/enright-srv/microcosm/htdocs/targets/v5/).

3′ UTR luciferase reporter assays

U251 cells were cotransfected with 100 ng psiCheck-2 RNF125 3′ UTR luciferase reporter plasmid or psiCheck-2 mutant RNF125 3′ UTR luciferase reporter plasmid, along with miR-15b mimics, inhibitors, or controls (final concentration, 50 nM). After 24 h, the cells were collected and assayed for reporter activity using the Dual-Luciferase Reporter System, following the manufacturer's instructions.

JEV infection and antagomir administration

Adult BALB/c mice (8 wk old) were purchased from the Hubei Provincial Center for Disease Control and Prevention (Wuhan, China). For miR-15b detection in mouse brain, mice were injected i.p. with 10^6 PFU JEV P3 strain in 200 μl PBS. The remaining mice were sacrificed on day 6 or day 23 postinfection, and brain samples were collected as described previously (38). For the antagomir studies, mice were randomly assigned to three groups: group 1, control group (PBS); group 2, the JEV-infected and antagomir control–treated group (JEV+Ctrl); and group 3, the JEV-infected and antagomir-15b–treated group (JEV+antagomir). Mice in groups 2 and 3 were inoculated intracranially with 200 PFU JEV P3 strain in 20 μl PBS (39), whereas mice in group 1 were injected intracranially with an equal volume of PBS. Twenty-four hours postviral infection, mice in groups 2 and 3 were administered antagomir control or antagomir-15b (60 mg/kg body weight, i.v.) on two consecutive days (40–42). After 5 d, mice infected with JEV developed signs of viral encephalitis; they were euthanized, and brain samples were collected for further studies. The remaining mice were monitored daily to assess behavior and mortality. All animal experiments were performed in accordance with the National Institutes of Health's *Guide for the Care and Use of Laboratory Animals*, and the experimental protocols were approved by the Research Ethics Committee of the College of Veterinary Medicine, Huazhong Agricultural University (No. S02914040M).

RNA extraction and quantitative real-time PCR

Total RNA was extracted from treated cells or mouse brain tissue with TRIzol reagent (Invitrogen), according to the manufacturer's instructions, and 1 μg RNA was used to synthesize cDNA with a first-strand cDNA synthesis kit (TOYOBO, Osaka, Japan). Quantitative real-time PCR (qRT-PCR) analysis was performed using a 7500 Real-time PCR System (Applied Biosystems) and SYBR Green PCR Master Mix (TOYOBO). Data were normalized according to the level of β-actin expression in each sample (43). Primers were as follows: human RNF125 forward, 5′-AGACAGGTGGTAGGCAAGTAGG-3′ and reverse, 5′-AACAA-

GAGCATTGGAGCAGATT-3′; human RIG-I forward, 5′-TTCCCACAAGGACAAAAG-3′ and reverse, 5′-GCCTGTAACTCTATACCCAT-3′; human IFN-β forward, 5′-TGCTCTGGCACAACAGGTAG-3′ and reverse, 5′-AGCCTCCCATTCAATTGCCA-3′; human ISG15 forward, 5′-ACAGCCATGGGCTGGGA-3′ and reverse, 5′-GATCTGCGCCTTCAGCTCT-3′; human ISG56 forward, 5′-AGCTTACACCATTGGCTGCT-3′ and reverse, 5′-CCATTTGTACTCATGGTTGCTGT-3′; human OAS1 forward, 5′-CTGGATTCTGCTGGCTGAAAG-3′ and reverse, 5′-CTGGAGTGTGCTGGGTCTATG-3′; human MxA forward, 5′-GGGCTTTGGAATTCTGTGGC-3′, and reverse, 5′-CCTTGGAATGGTGGCTGGAT-3′; human β-actin forward, 5′-AGCGGGAAATCGTGCGTGAC-3′ and reverse, 5′-GGAAGGAAGGCTGGAAGAGTG-3′; mouse RNF125 forward, 5′-CCGTGTTCATTCTGGCTTAGA-3′ and reverse, 5′-GCCTGTGTCGTGTCTCTTCC-3′; mouse IFN-β forward, 5′-AACTCCACCAGCAGACAGTG-3′ and reverse, 5′-GGTACCTTTGCACCCTCCAG-3′; mouse ISG15 forward, 5′-AGCAATGGCCTGGGACCTAAA-3′ and reverse, 5′-CAGACCCAGACTGGAAAGGG-3′; mouse ISG56 forward, 5′-ACCATGGGAGAGAATGCTGATG-3′ and reverse, 5′-TGTGCATCCCCAATGGGTTC-3′; mouse OAS1 forward, 5′-CTCTAAAGGGGTCAAGGGCA-3′ and reverse, 5′-TCTCTCATGCTGAACCTCGC-3′; mouse MxA forward, 5′-TCATCAGAGTGCAAGCGAGG-3′ and reverse, 5′-GGCTGTCTCCCTCTGATACG-3′; and mouse β-actin forward, 5′-CACTGCCGCATCCTCTTCCTCCC-3′ and reverse, 5′-CAATAGTGATGACCTGGCCGT-3′.

To quantify miR-15b levels, we used a commercial All-in-One miRNA qRT-PCR detection kit (GeneCopoeia). Briefly, 2 μg total RNA was used as the template and reverse transcribed using a miR-15b–specific stem-loop primer (5′-GTCGTATCCAGTGCAGGGTCCGAGGTATTCGCACTGGATACGACTGTAAA-3′). The resulting cDNA was subjected to qRT-PCR with a forward primer (5′-AGCAGCACATCATGGTTTAC-3′) and reverse primer (5′-GTGCAGGGTCCGAGGT-3′). Similarly, U6 small nuclear RNA was quantified using its reverse primer (5′-ATGGAACGCTTCACGAAT-3′) for the reverse-transcription reaction and its forward primer (5′-TCGGCAGCACATATACTAA-3′) and reverse primer for qRT-PCR. Amplification consisted of 2 min at 50°C and 5 min at 95°C, followed by 40 cycles of 95°C for 15 s, 60°C for 15 s, and 72°C for 30 s. The relative level of miR-15b was normalized to that of internal control U6 small nuclear RNA within each sample using the $2^{-\Delta\Delta Ct}$ method (43).

Western blotting

Total cellular lysates or mouse brain tissues lysates were generated by lysing cells in radioimmunoprecipitation assay buffer containing protease and phosphatase inhibitors (Roche, Mannheim, Germany). Protein concentrations were measured with a BCA Protein Assay Kit (Thermo Scientific). SDS-PAGE was performed, followed by protein transfer to polyvinylidene fluoride membranes using a Mini Trans-Blot Cell (Bio-Rad). Blots were probed with relevant Abs, and detection of proteins was conducted using ECL reagent (Thermo Scientific).

ELISA

The culture supernatants were collected from treated cells at the indicated time points and stored at −80°C. The protein levels of TNF-α, IL-1β, IL-6, CCL2, IL-12p70, and CCL5 in cell cultures or mouse brain tissue lysates were measured with ELISA kits (eBioscience), following the manufacturer's instructions.

H&E and immunohistochemical staining and TUNEL assay

Treated mice were anesthetized with ketamine-xylazine (0.1 ml/10 g body weight) and perfused with PBS, followed by 4% paraformaldehyde. Brain tissues were removed and embedded in paraffin for coronal sections. The sections were used for H&E and immunohistochemical (IHC) staining and TUNEL assays, as described previously (38). For IHC staining, sections were incubated overnight at 4°C with primary Abs against ionized calcium binding adapter molecule 1 (IBA-1; Wako, Osaka, Japan) or glial fibrillary acidic protein (GFAP; Dako, Glostrup, Denmark). After washing, slides were incubated with appropriate secondary Abs and washed, and diaminobenzidine (Vector Laboratories) was used for color development. For TUNEL, an In Situ Cell Death Detection Kit (Roche) was used, according to the manufacturer's instructions.

Statistical analysis

All experiments were repeated at least three times with similar results. Analyses were conducted using GraphPad Prism 5 (GraphPad Software, San Diego, CA). Results are expressed as mean ± SD. Data were compared with two-way ANOVA, with subsequent *t* tests using a Bonferroni posttest for multiple comparisons, or with a Student *t* test. For all tests, $p < 0.05$ was considered significant.

Results

Upregulation of miR-15b upon JEV infection

To determine the effect of JEV infection on the miRNA profile, a comprehensive deep-sequencing analysis of astrocyte U251 cells challenged with JEV was performed. Deep-sequencing data revealed that a group of miRNAs was differentially expressed upon JEV infection. Among these miRNAs, miR-15b was found to be significantly upregulated (>2-fold) following viral infection, and it was expressed at high levels in cells (data not shown). Because miR-15b was reported to be involved in chemokine- and cytokine-mediated inflammation pathways (44), it was selected for further characterization during JEV infection. Further validation of miR-15b expression patterns upon viral infection was analyzed in JEV-infected U251 cells using qRT-PCR. The results revealed that miR-15b levels were significantly elevated in a time- and dose-dependent manner (Fig. 1A, 1B). Furthermore, the expression of miR-15b in JEV-infected microglial cells (BV-2) was analyzed, which also showed significant time- and dose-dependent upregulation (Fig. 1C, 1D). We also investigated the expression of miR-15b in JEV-infected mouse brain samples. The results were similar to those observed in JEV-infected cell lines (Fig. 1E). These results strongly demonstrate that miR-15b expression is upregulated after JEV infection.

Effects of miR-15b on JEV-triggered inflammatory cytokine production

JEV-associated encephalitis is characterized by activation of resident glial cells and excessive production of inflammatory cytokines, which contributes to neuronal death (6, 45). To investigate whether miR-15b could affect the JEV-triggered inflammatory response, its effect on the regulation of inflammatory cytokine production after JEV challenge was assessed. First, the effects of synthetic miR-15b mimics and inhibitors on the expression of miR-15b were evaluated. miRNAs mimics are dsRNAs that are synthesized to simulate naturally occurring mature miRNAs, whereas inhibitors are chemically modified antisense ssRNAs that block the activity of endogenous miRNAs by complementarity. miRNA mimics and inhibitors can change the abundance of the physiological miRNAs. As expected, transfection of miR-15b mimics increased miR-15b levels significantly in mock- or JEV-infected U251 cells and BV-2 cells at 36 h postinfection, whereas miR-15b inhibitors reduced its levels (Fig. 2A, Supplemental Fig. 1A). In addition, the effects of miR-15b mimics and inhibitors on miR-15b levels were miR-15b specific, because no effect was observed on the levels of other miRNAs, such as miR-155 or miR–16-2 (data not shown). Interestingly, certain cytokines of JEV-associated neuroinflammation, including TNF-α, IL-1β, IL-6, CCL5, IL-12p70, and CCL2 (46), were significantly upregulated by the introduction of miR-15b mimics in both U251 cells (Fig. 2B) and BV-2 cells (Supplemental Fig. 1B). In contrast, the inhibition of endogenous miR-15b significantly decreased JEV-triggered cytokine production (Fig. 2B, Supplemental Fig. 1B). We further investigated the role of miR-15b in type I IFN and IFN-stimulated gene (ISG) expression induced by JEV. Similar to its effect on inflammatory cytokines, miR-15b increased JEV-induced production of IFN-β, ISG56, OAS1, MxA, and ISG15 in both U251 cells (Fig. 2C, 2D) and BV-2 cells (Supplemental Fig. 1C, 1D). Taken together, these data indicate that miR-15b is involved in the regulation of JEV-induced inflammation. Further, we found that treatment of miR-15b mimics or inhibitors did not show any antiviral capacity in JEV-infected U251 cells or BV-2 cells, because the viral load was equivalent to that in control cells (Fig. 2E, Supplemental Fig. 1E). Therefore, regulation of the JEV-induced inflammatory response by miR-15b was not due to changes in JEV replication.

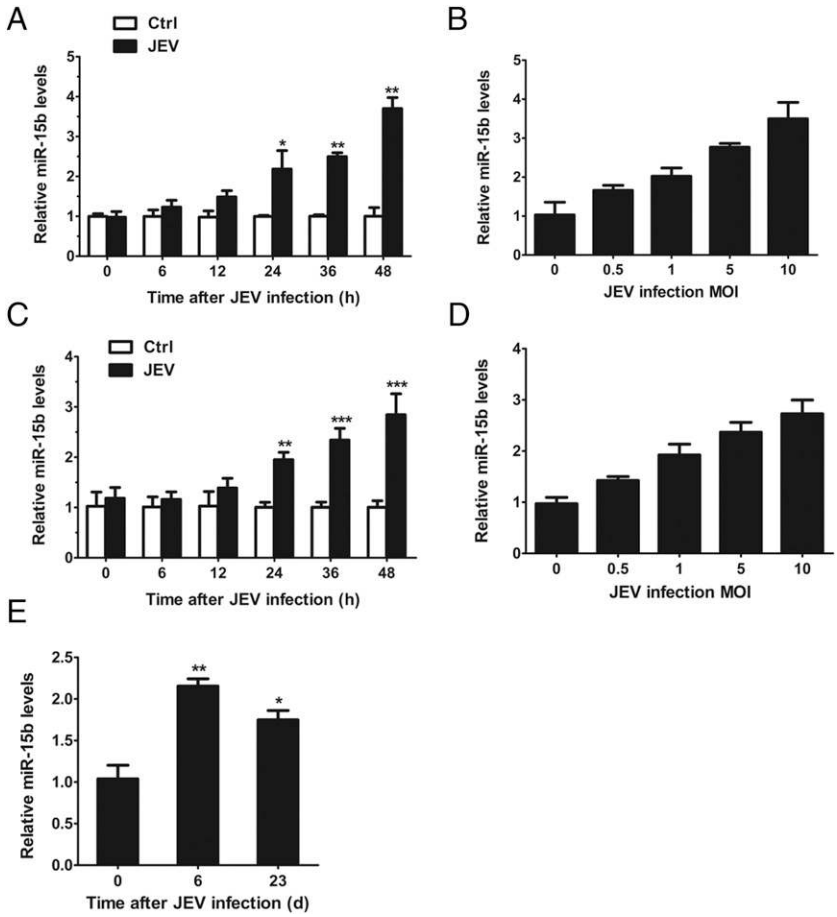

FIGURE 1. miR-15b expression is induced after JEV infection. U251 cells were infected with JEV at an MOI of 5 for the indicated times (**A**) or at the indicated MOIs for 36 h (**B**). The levels of miR-15b were detected by qRT-PCR. (**C** and **D**) Expression of miR-15b in JEV-infected BV-2 cells. All results were standardized to 1 in mock-infected cells for each group when qRT-PCR was performed. The data shown are representative of three independent experiments for in vitro study. $*p < 0.05$, $**p < 0.01$, $***p < 0.001$. (**E**) Expression of miR-15b in JEV-infected mouse brain. Mice were infected with JEV or mock infected with PBS, and brain samples were collected after 0, 6, or 23 d for analysis of miR-15b expression using qRT-PCR. The data are mean ± SD from three mice. $*p < 0.05$, $**p < 0.01$ versus day 0 (uninfected) mouse brain.

miR-15b targets RNF125

To understand the mechanism by which miR-15b regulates inflammation, the specific target of miR-15b was investigated further. By using several public miRNA target-prediction algorithms (47–49), RNF125, an important negative regulator of RIG-I, displayed potential seed matches for miR-15b. To confirm the possibility that RNF125 can be repressed posttranscriptionally by miR-15b, a luciferase reporter carrying a putative binding site along with a mutant construct containing the miR-15b target sequence with 4 bp mutations in the seed region were generated (Fig. 3A). A marked reduction in luciferase levels was found in U251 cells cotransfected with miR-15b mimics and wild-type RNF125 3′ UTR luciferase reporter plasmid, whereas significantly increased luciferase activity was observed following application of miR-15b inhibitors at 24 h posttransfection (Fig. 3B). Moreover, mutation of 4 bp in the miR-15b target sequence led to a complete abrogation of the negative effect of miR-15b on the expression of RNF125 3′ UTR reporter constructs (Fig. 3B). These results indicate that the nucleotide sequence in the 3′ UTR of RNF125 is a potential miR-15b targeting site. To further validate RNF125 as a target of miR-15b, the expression of endogenous RNF125 was examined in U251 cells treated with miR-15b mimics or inhibitors. As expected, the ectopic expression of miR-15b significantly suppressed RNF125 protein and mRNA levels (Fig. 3C), whereas the suppression of RNF125 could be restored in the presence of miR-15b inhibitors (Fig. 3D), suggesting that RNF125 expression could be inhibited by miR-15b via both translational repression and mRNA decay. Interestingly, like most known and functionally established miRNA binding sites, the miR-15b binding site within RNF125 3′ UTR was broadly conserved, whereas the miR-15b sequence itself is also conserved among vertebrates (Fig. 3E, 3F). Consistently, miR-15b also affected endogenous RNF125 expression at both the mRNA and protein levels in microglia BV-2 cells (Fig. 3G, 3H). Taken together, these data suggest that RNF125 is a direct target of miR-15b, and its expression is regulated by miR-15b.

miR-15b promotes RIG-I expression through suppression of RNF125

Previous studies showed that RNF125, a ubiquitin ligase, targets RIG-I for proteasomal degradation and, in turn, negatively regulates RIG-I signaling (34, 50, 51). To study the correlation between RNF125 and RIG-I during JEV infection, the expression patterns of RNF125 and RIG-I were determined. Following JEV infection, increased expression of RIG-I, as well as decreased expression of RNF125, was observed in a time-dependent manner (Fig. 4A). In contrast, the expression of RNF125 and RIG-I remained unchanged in cells inoculated with UV-inactivated JEV (Fig. 4A). These results, along with previous data, suggest that the expression of miR-15b and RIG-I is inversely correlated with RNF125 expression during JEV infection.

The repressive activity of miR-15b on its target, RNF125, becomes physiologically relevant if it is able to sustain the expression of RIG-I that is negatively modulated by RNF125. To test this hypothesis, the expression of RIG-I in mock- or JEV-infected U251 cells pretreated with miR-15b mimics or inhibitors was assessed. RIG-I expression was upregulated when miR-15b was overexpressed, and it was reduced when miR-15b was depleted (Fig. 4B). To better understand the role of miR-15b in RIG-I signaling, IRF3 and NF-κB activation was analyzed with miR-15b mimic or inhibitor treatment. Transfection of miR-15b mimics enhanced JEV-induced IRF3 phosphorylation and NF-κB p65 nuclear translocation. In contrast, treatment of cells with miR-15b inhibitors markedly attenuated the signals for

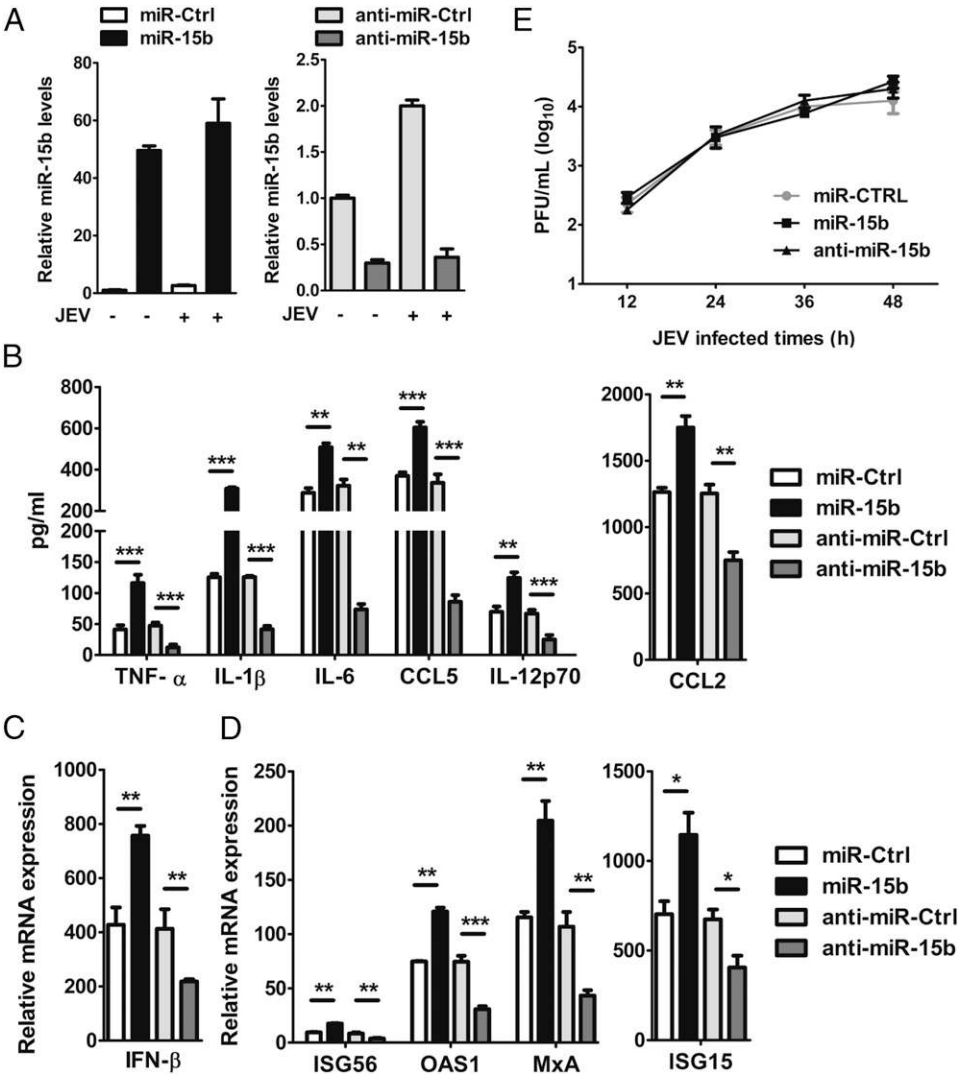

FIGURE 2. miR-15b is involved in regulating JEV-triggered inflammatory cytokine production. (**A**) U251 cells were transfected with mimics control (miR-Ctrl), miR-15b mimics (miR-15b), inhibitors control (anti–miR-Ctrl), or inhibitors (anti–miR-15b) for 24 h and then were left uninfected or infected with JEV at an MOI of 5 for 36 h. The level of miR-15b was analyzed by qRT-PCR and normalized to U6 level. (**B**) U251 cells were transfected as in (A) and infected with JEV at an MOI of 5 for 36 h. The protein levels of TNF-α, IL-1β, IL-6, CCL5, IL-12p70, and CCL2 were analyzed using ELISA. Data are mean ± SD from three independent experiments performed in duplicate. (**C** and **D**) U251 cells were treated as described in (B), and the levels of IFN-β, ISG56, OAS1, MxA, and ISG15 were determined by qRT-PCR. The expression of each target gene was normalized to β-actin. Data are mean ± SD from three independent experiments. (**E**) The transfected U251 cells were infected with JEV at an MOI of 5. Cells were collected at the indicated time points, and titers of infectious virus in the culture supernatants were detected by plaque assay. The data represent three independent experiments with identical results. $*p < 0.05$, $**p < 0.01$, $***p < 0.001$.

IRF3 and NF-κB activation (Fig. 4B, 4C). These observations suggest that miR-15b could enhance the expression level of RIG-I and promote RIG-I signaling during JEV infection.

To further substantiate that miR-15b is involved in the regulation of RIG-I via RNF125, U251 cells were cotransfected with miR-15b mimics and RNF125 expression vector with WT or mutant 3′ UTR, and the expression of RIG-I was determined in both mock- and JEV-infected cells. As shown in Fig. 4D, overexpression of miR-15b enhanced the levels of RIG-I in cells transfected with WT RNF125, whereas RNF125 with mutant 3′ UTR decreased miR-15b responsiveness. A similar enhancement of JEV-induced activation of IRF3 and NF-κB by miR-15b was observed in cells overexpressing RNF125 with WT 3′ UTR. However, when ectopically introduced, RNF125 with mutant 3′ UTR rescued miR-15b–mediated activation of IRF3 and NF-κB (Fig. 4D, 4E).

To establish the proteasome-mediated disintegration of RIG-I via RNF125, RIG-I protein and mRNA were detected in cells transfected with RNF125, followed by MG132 (a proteasome inhibitor) treatment. As illustrated in Fig. 4F, RIG-I expression was reduced in cells transfected with RNF125. When cells were treated with MG132, the level of RIG-I expression was partially restored (Fig. 4F). However, mRNA levels of RIG-I remained unchanged (Fig. 4F). Next, we examined whether miR-15b could inhibit degradation of RIG-I. As shown in Fig. 4G, knockdown of endogenous miR-15b by specific inhibitors reduced the levels of RIG-I, but this effect was reverted when cells were treated with MG132 (Fig. 4G). These results suggest that miR-15b inhibitors reduce the levels of RIG-I through proteasomal degradation. Therefore, there is a specific relationship between miR-15b and RIG-I during JEV infection: miR-15b–mediated RNF125 repression leads to positive regulation of RIG-I signaling.

miR-15b regulates JEV-induced inflammatory cytokine expression via targeting RNF125

To determine whether the observed effects of miR-15b on inflammatory cytokine production in response to JEV infection were mediated, at least in part, through RNF125, we analyzed the effects of overexpression of RNF125 with intact or mutant 3′ UTR in U251 cells and BV-2 cells. The results showed that the addition of miR-15b mimics increased JEV-triggered production of TNF-α, IL-1β, IL-6, CCL5, IL-12p70, and CCL2 in U251 cells and BV-2 cells transfected with RNF125 harboring the WT 3′ UTR plasmid. Of note, miR-15b–mediated proinflammatory effects were abrogated by overexpressed RNF125 with mutated 3′ UTR in U251 cells and BV-2 cells (Fig. 5A, Supplemental Fig. 2A). However, treatment of miR-15b mimics did not change the viral load in U251 cells and BV-2 cells overexpressing RNF125 (Fig. 5B, Supplemental Fig. 2B). To further verify the role of RNF125 in the JEV-induced inflammatory response, the effects of silencing RNF125 expression by siRNA were analyzed in U251 cells and BV-2 cells. Knockdown of RNF125 significantly increased the JEV-induced production of

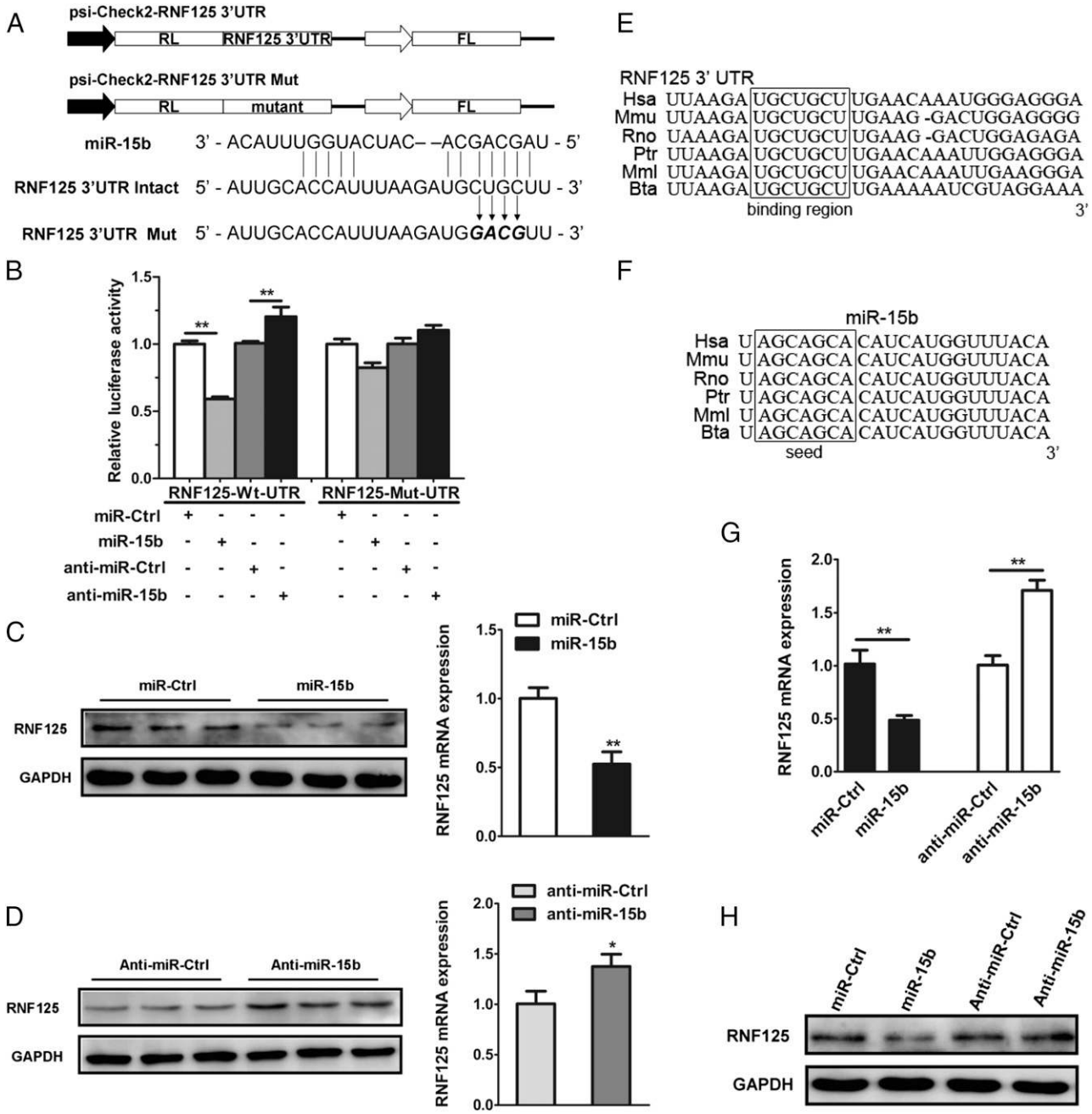

FIGURE 3. miR-15b directly targets RNF125. (**A**) Schematic diagram showing 3′ UTR of RNF125 luciferase reporter constructs containing the putative miR-15b binding site. The alignment of miR-15b and its target site in the 3′ UTR of RNF125 are shown below. Four mutated nucleotides of the target site are indicated in bold italic type. (**B**) U251 cells were transfected with miR-15b mimics, miR-15b inhibitors, or their control oligonucleotides along with a WT or mutated RNF125 3′ UTR luciferase reporter plasmid and assessed for luciferase activity at 24 h after transfection. Data are presented as relative *Renilla* luciferase activities normalized to the value of firefly luciferase. Similar results were obtained in three independent experiments. (**C** and **D**) U251 cells were transfected with miR-15b mimics or inhibitors for 48 h. RNF125 protein levels and mRNA levels were measured by Western blotting and qRT-PCR, respectively. Similar results were obtained in three independent experiments. (**E**) Alignment of RNF125 3′ UTR from different species for the miR-15b binding region. (**F**) Alignment of miR-15b seed sequence from different species. (**G** and **H**) BV-2 cells were transfected with miR-15b mimics, miR-15b inhibitors, or their control oligonucleotides for 48 h. The levels of RNF125 mRNA and RNF125 protein were determined. In all experiments, control oligonucleotides were used as a transfection control. Similar results were obtained in three independent experiments. $*p < 0.05$, $**p < 0.01$, Student *t* test.

inflammatory cytokines, which produce effects similar to those of miR-15b overexpression. In line with previous data, JEV-induced expression of TNF-α, IL-1β, IL-6, CCL5, IL-12p70, and CCL2 was decreased by anti–miR-15b. Importantly, silencing of RNF125 rescued the suppressive effect of anti–miR-15b on these cytokines (Fig. 5C, Supplemental Fig. 2C). JEV replication was repressed by knockdown of RNF125, but this effect was not changed in the presence of anti–miR-15b in U251 cells (Fig. 5D) or BV-2 cells (Supplemental Fig. 2D). These results suggest that silencing of RNF125 phenocopied the proinflammatory effect of miR-15b and counteracted the effect of anti–miR-15b.

Because RNF125 is a direct target of miR-15b, and RNF125 negatively regulates RIG-I signaling, we tested whether altering the abundance of RIG-I influenced the effect of miR-15b on the cytokine production induced by JEV. Knockdown of RIG-I in cells expressing mimics control markedly reduced the cytokine

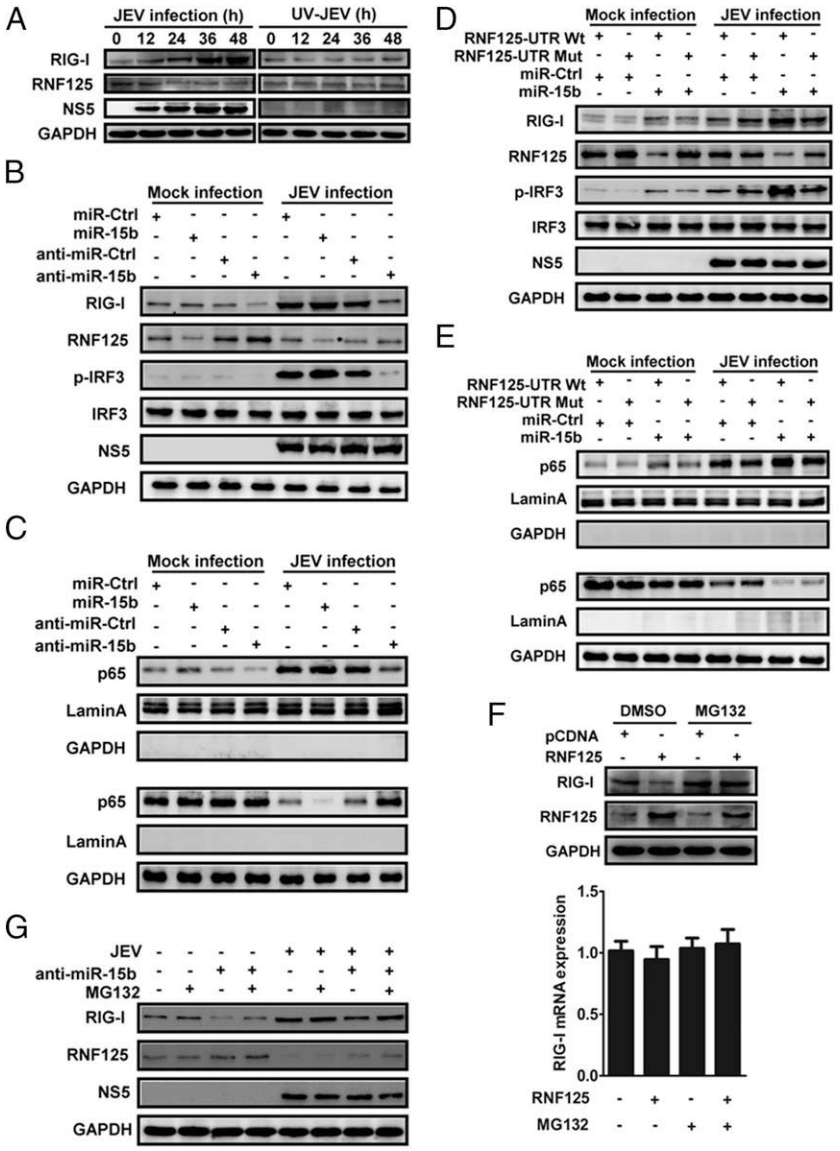

FIGURE 4. miR-15b–induced expression of RIG-I is mediated by RNF125. (**A**) U251 cells were infected with JEV (*left panel*) or UV-inactivated JEV (*right panel*) over a 48-h time course and harvested at the indicated time points. The levels of RIG-I, RNF125, and JEV NS5 protein were detected by Western blotting, using GAPDH as a loading control. (**B** and **C**) U251 cells were transfected with miR-15b mimics or inhibitors for 24 h and then infected with medium or JEV for another 24 h. (B) The levels of RIG-I, RNF125, p-IRF3, IRF3, NS5, and GAPDH in the whole-cell lysates were monitored by immunoblotting. (C) The nuclear extracts (*upper panel*) and cytosolic extracts (*lower panel*) were isolated and subjected to immunoblotting with Abs against NF-κB p65, Lamin A, and GAPDH. Lamin A was used as a marker for nuclei. GAPDH and Lamin A were used as loading controls. (**D** and **E**) U251 cells were cotransfected with miR-15b mimics and RNF125 expression vector with WT or mutant 3′ UTR for 24 h and were either left uninfected or infected with JEV. (D) The levels of RIG-I, RNF125, p-IRF3, IRF3, NS5, and GAPDH in the whole-cell lysates were detected by immunoblotting. (E) The nuclear extracts (*upper panel*) and cytosolic extracts (*lower panel*) were isolated and subjected to immunoblotting with Abs against NF-κB p65, Lamin A, and GAPDH. (**F**) U251 cells were transfected with pCDNA or pCDNA-RNF125 for 24 h. Then cells were treated with MG132 (20 nM) or DMSO for 8 h before collecting samples. The levels of RIG-I protein (*upper panel*) and mRNA (*lower panel*) were detected by Western blotting and qRT-PCR, respectively. (**G**) U251 cells were transfected with miR-15b inhibitors or control inhibitors for 24 h and then infected with medium or JEV for another 24 h. Cells were treated with MG132 (20 nM) or DMSO for 8 h before collecting samples. The levels of RIG-I, RNF125, and NS5 were detected by Western blotting. All of the blots are a representative of three experiments with similar results.

production induced by JEV. More importantly, the miR-15b–mediated proinflammatory effect was inhibited in cells transfected with RIG-I siRNA (Fig. 5E, Supplemental Fig. 2E). In addition, treatment with RIG-I–specific siRNA led to an increase in viral load, which was not affected by miR-15b (Fig. 5F, Supplemental Fig. 2F). Collectively, these results demonstrate that virally induced miR-15b regulates JEV-triggered cytokine production through suppression of endogenous RNF125.

Antagomir-15b treatment regulates neuroinflammation and lethality in JEV-infected mice

To characterize the role of miR-15b in JEV-induced encephalitis in vivo, a mouse model of JEV infection was established. A chemically modified antisense oligonucleotide specific for miR-15b (antagomir-15b) was delivered to mice via tail vein injections at 24 h post-JEV infection to silence endogenous miR-15b expression. This chemically modified antagomir can cross the blood–brain barrier into the CNS via i.v. routes, as described previously (40, 41). Mice tolerated antagomir-15b well, without signs of illness or discomfort. Five days postinfection, JEV-infected mice developed typical symptoms, including restriction of movement, limb paralysis, and marked ataxia. Mice were sacrificed, and brain tissues were collected for further experiments.

Consistent with the in vitro data, brain samples from JEV-infected mice showed a reciprocal correlation between miR-15b levels and the expression of RNF125: higher miR-15b expression was associated with lower expression of RNF125 (Fig. 6A–C). In JEV-infected mice, antagomir-15b treatment resulted in specific inhibition of miR-15b expression (Fig. 6A) and reversed changes in RNF125 expression (Fig. 6B, 6C). The expression of RNF125 was verified with IHC staining in the mouse brain (Fig. 6D). Furthermore, we found that inflammatory cytokines, including IL-1β, IL-6, and CCL2, were increased significantly after JEV-infected mice were treated with the control antagomir, whereas these cytokine levels were attenuated by antagomir-15b treatment (Fig. 6E). Because inflammatory cytokines are responsible for the cytotoxic and neuropathological conditions during JEV infection (45, 52), reduced cytokine levels following antagomir-15b treatment would be helpful for limiting neuronal death.

At day 5 postinfection, brain sections from mice challenged with JEV or PBS were examined for pathological changes. Brains of antagomir control–treated mice showed the typical histopathological features of viral encephalitis, whereas pathological alterations were alleviated by antagomir-15b treatment (Fig. 7A). Moreover, JEV infection caused astrocytosis and microgliosis. An abnormal increase in the number of astrocytes and microglias was detected by IHC

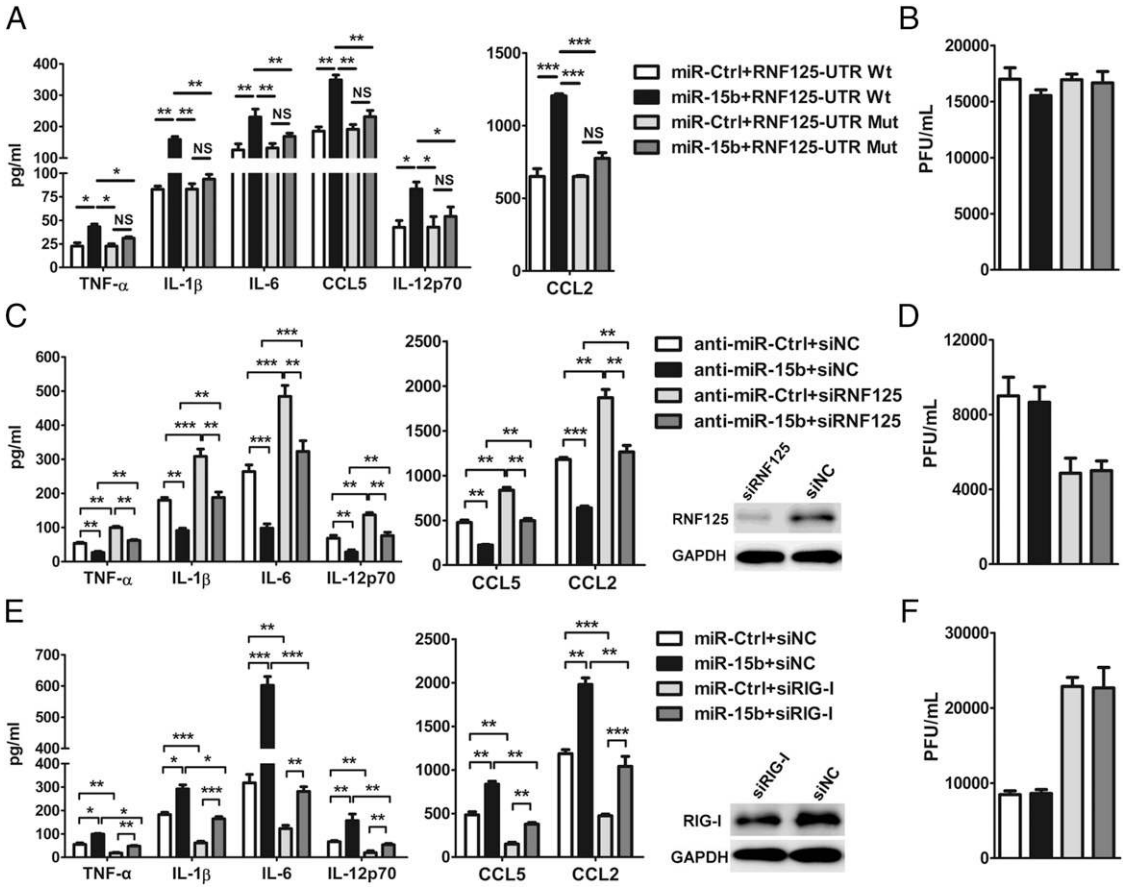

FIGURE 5. Regulation of JEV-triggered inflammatory cytokine production by miR-15b is achieved through RNF125. (**A** and **B**) U251 cells were cotransfected with miR-15b mimics and RNF125 expression vector with WT or mutant 3′ UTR for 24 h and then infected with JEV. At 36 h postviral infection, TNF-α, IL-1β, IL-6, CCL5, IL-12p70, and CCL2 secretion was detected by ELISA. The titers of infectious virus in the culture supernatants were detected by plaque assay. (**C** and **D**) U251 cells were cotransfected with miR-15b inhibitors or inhibitors control and siRNA against RNF125 or nonspecific control siRNA, as indicated, for 24 h and then infected with JEV. At 36 h postviral infection, cytokines and viral titers were determined by ELISA and plaque assay, respectively. (**E** and **F**) U251 cells were transiently cotransfected with control or miR-15b mimics together with control siRNA or RIG-I siRNA for 24 h. At 36 h postviral infection, the cytokines and viral titers were analyzed by ELISA and plaque assay, respectively. In all experiments, similar results were obtained in three independent experiments. $*p < 0.05$, $**p < 0.01$, $***p < 0.001$.

staining using GFAP and IBA-1. Plentiful star-shaped, activated astrocytes were observed in the antagomir control–treated group, whereas antagomir-15b treatment significantly downregulated astrocyte proliferation (Fig. 7B). Similarly, reactive microgliosis was decreased in the antagomir-15b–treated group (Fig. 7C). To determine whether antagomir-15b could reduce neuronal damage, brain sections were processed for TUNEL assay. The number of surviving cells was increased significantly with antagomir-15b treatment in JEV-infected mice compared with antagomir control–treated mice (Fig. 7D). These results suggest that antagomir-15b treatment could reduce the activation of astrocytes and microglia and prevent neuronal death.

Based on reduced neuroinflammation in antagomir-15b–treated JEV-infected mice, we next evaluated the potential of antagomir-15b to protect against a lethal intracranial challenge with JEV. High mortality was observed in mice that succumbed to JEV infection 6 d postinfection (Fig. 7E). All mice in the PBS groups survived. JEV challenge in the antagomir control treatment group resulted in typical symptoms of viral encephalitis, and all mice died by the sixth day. In contrast, administration of antagomir-15b protected mice from early lethality (within 5 d postinfection), and 60% of mice survived for the entire 23-d observation period (Fig. 7E). Due to the difference in mortality between antagomir control treatment and antagomir-15b treatment, viral titers in the brain were measured by plaque assays. Brain homogenates from antagomir control–treated mice revealed high levels of viral replication, whereas the homogenates from antagomir-15b–treated mice showed lower levels of viral titers (Fig. 7F). Taken together, the reduction in neuroinflammation and viral titers in antagomir-15b–treated mice could explain the improved survival seen in JEV-infected mice. Thus, our study demonstrates therapeutic efficacy for silencing of miR-15b by antagomir-15b in JEV-induced neuroinflammation and lethality.

Discussion

Neuroinflammation with activation of glial cells and neural infiltration of peripheral immune cells is a common feature of Japanese encephalitis (6, 52). Following JEV invasion, glial cells play an essential role in the immune response against pathogens; however, viral replication within glial cells leads to bystander neuronal death by secretion of inflammatory mediators (6). miRNAs have emerged as a major class of gene-expression regulators implicated in the immune response during inflammation and/or infections (17, 18). Thus, in this study, we aimed to address the role of miRNA-regulated pathways in the JEV-induced neuroinflammation model. Recently, the roles of miR-29b and miR-155 in microglial activation during JEV-induced neuroinflammation were studied (42, 53, 54). In this study, we demonstrated that miR-15b is stimulated both in vitro and in vivo, and miR-15b regulates the inflammatory response following JEV infection by targeting RNF125.

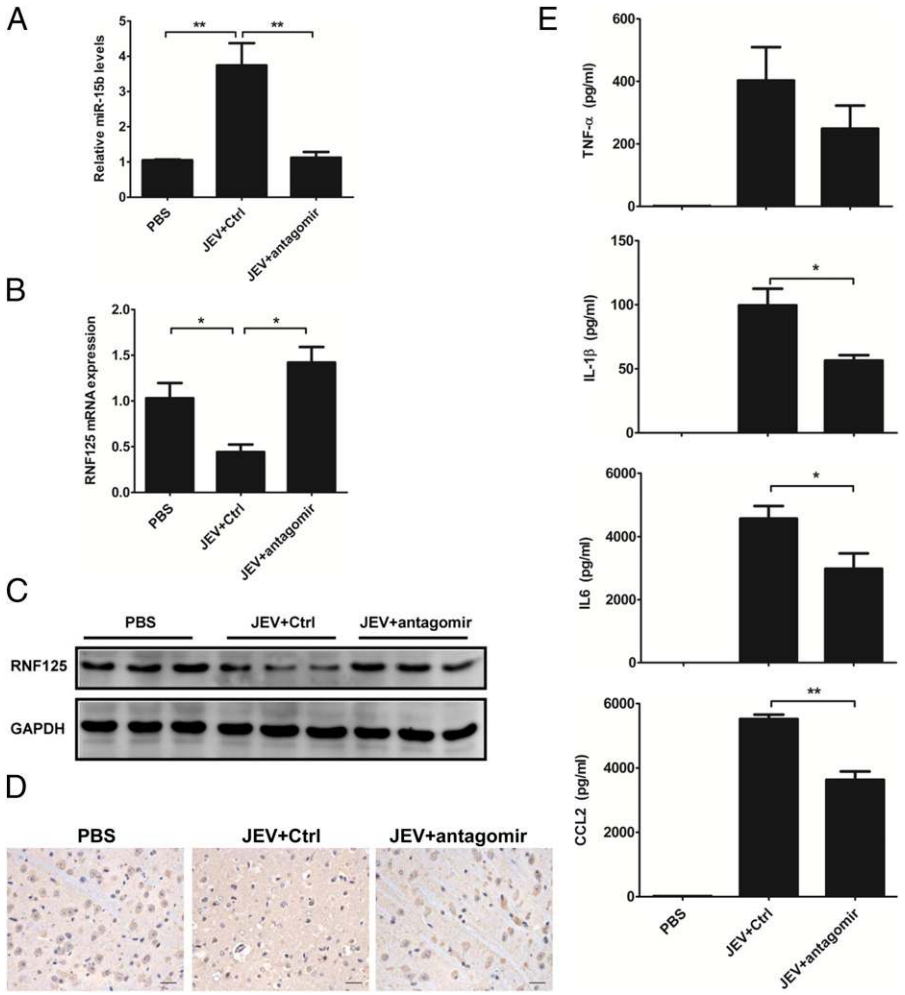

FIGURE 6. Antagomir-15b treatment restores RNF125 expression and attenuates the production of inflammatory cytokines in the JEV-infected mouse model. Mice were treated with antagomir control or antagomir-15b (60 mg/kg) after JEV infection, and brain samples were collected at day 5 postviral infection. (**A**) The increase in miR-15b expression was neutralized in JEV-infected mice by administration of antagomir-15b. (**B** and **C**) Suppression of RNF125 was restored by antagomir-15b injection in JEV-infected mice. RNF125 mRNA and protein levels were evaluated by qRT-PCR and Western blotting, respectively. (**D**) RNF125 expression was evaluated using IHC staining of brain sections from JEV-infected mice treated with antagomir control, antagomir-15b, or PBS (scale bars, 100 μm). (**E**) Antagomir-15b treatment decreased the production of cytokines. The levels of TNF-α, IL-1β, IL-6, and CCL2 in brain samples were detected by ELISA. Similar results were obtained in three mice. $*p < 0.05$, $**p < 0.01$, two-tailed Student t test. JEV+antagomir, samples collected from JEV-infected mice treated with antagomir-15b; JEV+Ctrl, samples collected from JEV-infected mice treated with antagomir control; PBS, samples collected from PBS-challenged mice.

miR-15b was found to be highly expressed in hepatocellular carcinoma (26) and other tumors (27), indicating its potential importance in cancers. miR-15b promotes HBV replication by targeting HNF1α, and miR-15b expression in hepatocytes is downregulated by HBV in the early stages of HBV infection (30). In this study, modulation of JEV-induced inflammatory cytokine production could be a novel function of miR-15b, suggesting that the miRNA regulates tumor cell apoptosis, as well as regulates inflammation and innate immune responses.

miRNAs function primarily by binding to the 3′ UTR of target mRNAs to achieve posttranscriptional regulation of gene expression (12). Several studies showed that miRNAs regulate genes related to inflammatory pathways following JEV infection. miR-29b is a potent regulator of JEV-induced neuroinflammation by the targeting of TNFAIP3, a negative regulator of NF-κB signaling in microglia cells (54). miR-155 modulates the neuroinflammatory response during JEV infection via negative regulation of SHIP1 expression (42). Consistently, we found that miR-15b also participates in the JEV-associated inflammatory response. The molecular mechanisms by which miR-15b regulates inflammatory cytokine production during JEV infection were explored in the current study. Because miR-15b is overexpressed during JEV infection, and miR-15b functions as a positive regulator of the inflammatory response, we hypothesize that miR-15b represses important suppressors in inflammatory signaling. In this study, we found that miR-15b directly targets RNF125, which was shown to be a negative regulator of RIG-I signaling (34, 51). Our data showed that miR-15b markedly inhibits RNF125 expression and promotes the production of inflammatory cytokines by the regulation of RNF125. Furthermore, RNF125 with mutated 3′ UTR overexpression abrogated miR-15b–mediated proinflammatory effects on JEV-treated glial cells, suggesting that RNF125 is a target of miR-15b in the modulation of JEV-induced production of inflammatory cytokines. Although we showed that RNF125 was targeted by miR-15b to regulate the JEV-induced inflammatory response, RNF125 is not the only target of miR-15b. Given that RIG-I plays essential roles in JEV-induced inflammation (46, 55, 56), we focused our current study on miR-15b–regulated RIG-I pathways. Further exploration of other potential targets of miR-15b and more detailed mechanisms are required in future studies.

RIG-I, a cytoplasmic sensor for viral RNA, was shown to be essential in the mediation of the proinflammatory response following JEV infection (46, 55, 56). Many proteins are known to modify the RIG-I pathway and the subsequent cytokine signal transduction (34, 51, 57, 58), but the role of miRNA-mediated regulation is only beginning to emerge. Thus, the level of receptor expression is the first and likely effective point at which miRNAs exert their functions, but few studies have focused on the regulation of RIG-I expression by miRNAs (18). In this study, JEV infection induced miR-15b expression, and miR-15b increased JEV-induced expression of RIG-I, coincident with enhanced IRF3 signaling and NF-κB signaling, by targeting a regulon of RIG-I, RNF125. Therefore, we report the discovery of a potentially new class of RIG-I regulators: miR-15b. In addition, knockdown of miR-15b decreased RIG-I expression, but the negative effects of miR-15b inhibitors on RIG-I expression

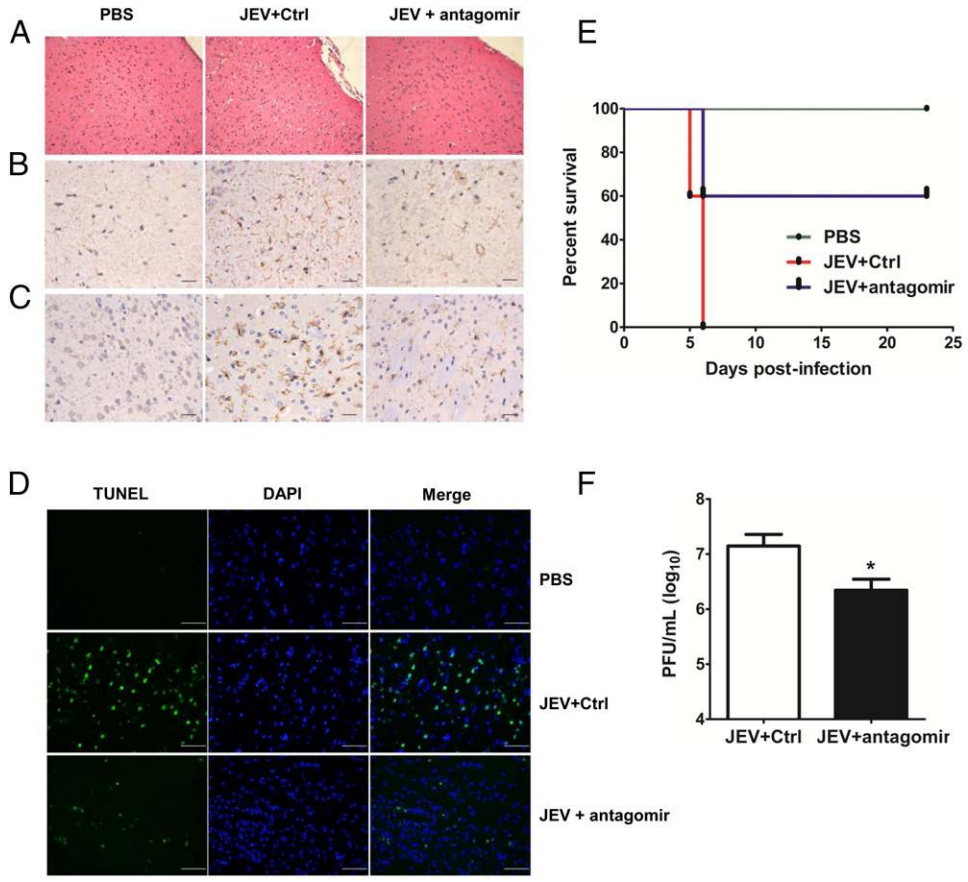

FIGURE 7. Antagomir-15b treatment alleviates neuroinflammation and improves survival in JEV-challenged mice. (**A**) Antagomir-15b treatment improves histopathological changes in mice caused by JEV. H&E staining of brain sections was performed to observe pathological changes. Scale bars, 50 μm. (**B** and **C**) Antagomir-15b treatment reduces astrocytosis and microgliosis. Sections of brain were analyzed by IHC staining. (B) Activation of astrocytes was detected by anti-GFAP Ab. (C) Activation of microglia was detected by IHC staining with anti–IBA-1 Ab. Scale bars, 100 μm. (**D**) Antagomir-15b treatment decreases neuronal damage. The apoptotic cells in the brain sections were stained using the TUNEL assay kit. Scale bars, 100 μm. The figures are a representative of three mice with similar results. (**E**) Antagomir-15b treatment improves survival. Survival of mice in each group was monitored for 23 d after intracranial injection with JEV (200 PFU/mice). Data were collected and are shown as Kaplan–Meier survival curves ($n = 5$ mice). (**F**) Viral titers in brain isolated from mice treated with antagomir at day 5 post-JEV challenge were determined by plaque assay. The viral titers are shown as log PFU/ml ($n = 3$ mice). $^*p < 0.05$, Student unpaired t test.

were restored by MG132 treatment, suggesting that miR-15b enhances RIG-I expression by targeting RNF125 during JEV infection, which might be due to inhibition of RIG-I proteasomal degradation through ubiquitination.

Given that miR-15b modulates JEV-induced IFN-β, as well as downstream ISG, mRNA expression, we investigated the biological significance of virally induced miR-15b upregulation by measuring JEV replication. Interestingly, we found that miR-15b did not limit JEV replication in glial cells. Thounaojam et al. (42) showed similar results: JEV-induced miR-155 increased TBK1, IRF3/7, and NF-κB phosphorylation and IFN-β expression, but it did not alter the viral load following JEV infection. They also reported that miR-29b has a proinflammatory role during JEV-induced microglial activation. They observed nonsignificant changes in viral load after transfection with anti–miR-29b or miR-29b mimic compared with JEV alone (54). Additionally, miR-451 knockdown increased IFN-β production and a panel of ISG expression during influenza infection, but it did not impact dendritic cell antiviral capacity (59). This observation might be explained by the fact that the expression levels of IFN-β and ISGs induced by miR-15b may not be enough to exert effects on JEV replication. Another explanation for the observed viral replication phenotype is that JEV may evade the cellular immune response; however, the possibility needs to be addressed in our future studies.

It was reported that glial cells are activated during JEV invasion (52), leading to the production of numerous inflammatory cytokines, such as TNF-α, IL-1β, IL-6, CCL2, and CCL5. The increased levels of inflammatory mediators initiate an irreversible immune response, leading to neuronal cell death (52). Therefore, suppression of the extensive inflammatory response could potentially halt the progression of events, leading to mortality and morbidity caused by JEV infection, and it seems to be a practical and curative measure against JEV infection (38, 42, 60). In this regard, a JEV-infected mouse model was established to validate the effects of miR-15b in vivo. In JEV-infected mouse brain, RNF125 showed a reciprocal expression pattern with miR-15b, which further supports a functional interaction between mRNA and miRNA in vivo. Antagomir-15b treatment in an early stage of virus infection has inhibitory effects on cytokine release in JEV-infected mice; it can inhibit the activation of microglia and astrocytes and reduce neuronal death. After antagomir-15b treatment, ∼60% of JEV-infected mice became asymptomatic and survived for ≥23 d postinfection, whereas the antagomir control–treated mice remained weak and died gradually within 6 d. Our results indicate that JEV-induced neuroinflammation is the key factor in predicting the progression of JEV infection and that suppression of neuroinflammation in the acute stage is critical to improve survival.

Using in vivo data, we showed that inhibition of miR-15b resulted in a reduction in brain viral titers. Compared with its anti-inflammatory property, the antiviral effect of antagomir-15b in mouse brain is an interesting phenomenon. It seems unlikely that antagomir-15b has antiviral activity, because inhibition of miR-15b did not alter viral replication in U251 cells or BV-2 cells. We propose that, rather than exerting direct antiviral activity, antagomir-15b modifies the inflammatory environment by reducing neuroinflammation and neuronal death, which, in turn, may benefit the host by clearing virus and increasing protection against JEV. Consistently, several studies also reported that impairment of inflammatory cytokine production during JEV infection with minocycline (61) or rosmarinic acid (62) can increase neuroprotection and decrease viral replication (63).

In summary, this study provides direct evidence for the association of miR-15b with the JEV-induced inflammatory response, and miR-15b plays a role as a positive regulator in constraining the production of proinflammatory cytokines induced by JEV in vitro and in vivo. Additionally, we observed that RNF125 is a novel target for miR-15b, and miR-15b acts as a regulator of RIG-I. Finally, neutralization of virus-induced miR-15b could attenuate neuroinflammation, thereby relieving symptoms and reducing mortality in the mouse model. Therefore, inhibition of miR-15b may be an attractive candidate for the development of new therapeutic interventions. Moreover, this study may also provide insight into the use of miRNA-based therapeutics against other neuroinflammation-related diseases.

Disclosures

The authors have no financial conflicts of interest.

References

1. Cook, D. N., D. S. Pisetsky, and D. A. Schwartz. 2004. Toll-like receptors in the pathogenesis of human disease. *Nat. Immunol.* 5: 975–979.
2. Misra, U. K., and J. Kalita. 2010. Overview: Japanese encephalitis. *Prog. Neurobiol.* 91: 108–120.
3. van den Hurk, A. F., S. A. Ritchie, and J. S. Mackenzie. 2009. Ecology and geographical expansion of Japanese encephalitis virus. *Annu. Rev. Entomol.* 54: 17–35.
4. Mackenzie, J. S., D. J. Gubler, and L. R. Petersen. 2004. Emerging flaviviruses: the spread and resurgence of Japanese encephalitis, West Nile and dengue viruses. *Nat. Med.* 10(12, Suppl.)S98–S109.
5. Erlanger, T. E., S. Weiss, J. Keiser, J. Utzinger, and K. Wiedenmayer. 2009. Past, present, and future of Japanese encephalitis. *Emerg. Infect. Dis.* 15: 1–7.
6. Ghoshal, A., S. Das, S. Ghosh, M. K. Mishra, V. Sharma, P. Koli, E. Sen, and A. Basu. 2007. Proinflammatory mediators released by activated microglia induces neuronal death in Japanese encephalitis. *Glia* 55: 483–496.
7. Chen, C. J., J. H. Chen, S. Y. Chen, S. L. Liao, and S. L. Raung. 2004. Up-regulation of RANTES gene expression in neuroglia by Japanese encephalitis virus infection. *J. Virol.* 78: 12107–12119.
8. Chen, C. J., S. L. Liao, M. D. Kuo, and Y. M. Wang. 2000. Astrocytic alteration induced by Japanese encephalitis virus infection. *Neuroreport* 11: 1933–1937.
9. Olson, J. K., and S. D. Miller. 2004. Microglia initiate central nervous system innate and adaptive immune responses through multiple TLRs. *J. Immunol.* 173: 3916–3924.
10. Thongtan, T., P. Cheepsunthorn, V. Chaiworakul, C. Rattanarungsan, N. Wikan, and D. R. Smith. 2010. Highly permissive infection of microglial cells by Japanese encephalitis virus: a possible role as a viral reservoir. *Microbes Infect.* 12: 37–45.
11. Bhowmick, S., R. Duseja, S. Das, M. B. Appaiahgiri, S. Vrati, and A. Basu. 2007. Induction of IP-10 (CXCL10) in astrocytes following Japanese encephalitis. *Neurosci. Lett.* 414: 45–50.
12. Bartel, D. P. 2004. MicroRNAs: genomics, biogenesis, mechanism, and function. *Cell* 116: 281–297.
13. Friedman, R. C., K. K. Farh, C. B. Burge, and D. P. Bartel. 2009. Most mammalian mRNAs are conserved targets of microRNAs. *Genome Res.* 19: 92–105.
14. Chen, J. F., E. M. Mandel, J. M. Thomson, Q. Wu, T. E. Callis, S. M. Hammond, F. L. Conlon, and D. Z. Wang. 2006. The role of microRNA-1 and microRNA-133 in skeletal muscle proliferation and differentiation. *Nat. Genet.* 38: 228–233.
15. Lu, J., G. Getz, E. A. Miska, E. Alvarez-Saavedra, J. Lamb, D. Peck, A. Sweet-Cordero, B. L. Ebert, R. H. Mak, A. A. Ferrando, et al. 2005. MicroRNA expression profiles classify human cancers. *Nature* 435: 834–838.
16. Guo, C. J., Q. Pan, D. G. Li, H. Sun, and B. W. Liu. 2009. miR-15b and miR-16 are implicated in activation of the rat hepatic stellate cell: An essential role for apoptosis. *J. Hepatol.* 50: 766–778.
17. Cullen, B. R. 2013. MicroRNAs as mediators of viral evasion of the immune system. *Nat. Immunol.* 14: 205–210.
18. Li, Y., and X. Shi. 2013. MicroRNAs in the regulation of TLR and RIG-I pathways. *Cell. Mol. Immunol.* 10: 65–71.
19. Hou, J., P. Wang, L. Lin, X. Liu, F. Ma, H. An, Z. Wang, and X. Cao. 2009. MicroRNA-146a feedback inhibits RIG-I-dependent type I IFN production in macrophages by targeting TRAF6, IRAK1, and IRAK2. *J. Immunol.* 183: 2150–2158.
20. Chen, Y., J. Chen, H. Wang, J. Shi, K. Wu, S. Liu, Y. Liu, and J. Wu. 2013. HCV-induced miR-21 contributes to evasion of host immune system by targeting MyD88 and IRAK1. *PLoS Pathog.* 9: e1003248.
21. Lu, F., A. Weidmer, C. G. Liu, S. Volinia, C. M. Croce, and P. M. Lieberman. 2008. Epstein-Barr virus-induced miR-155 attenuates NF-kappaB signaling and stabilizes latent virus persistence. *J. Virol.* 82: 10436–10443.
22. Taganov, K. D., M. P. Boldin, K. J. Chang, and D. Baltimore. 2006. NF-kappaB-dependent induction of microRNA miR-146, an inhibitor targeted to signaling proteins of innate immune responses. *Proc. Natl. Acad. Sci. USA* 103: 12481–12486.
23. Ceppi, M., P. M. Pereira, I. Dunand-Sauthier, E. Barras, W. Reith, M. A. Santos, and P. Pierre. 2009. MicroRNA-155 modulates the interleukin-1 signaling pathway in activated human monocyte-derived dendritic cells. *Proc. Natl. Acad. Sci. USA* 106: 2735–2740.
24. Chen, Y., W. Liu, T. Sun, Y. Huang, Y. Wang, D. K. Deb, D. Yoon, J. Kong, R. Thadhani, and Y. C. Li. 2013. 1,25-Dihydroxyvitamin D promotes negative feedback regulation of TLR signaling via targeting microRNA-155-SOCS1 in macrophages. *J. Immunol.* 190: 3687–3695.
25. Yue, J., and G. Tigyi. 2010. Conservation of miR-15a/16-1 and miR-15b/16-2 clusters. *Mamm. Genome* 21: 88–94.
26. Chung, G. E., J. H. Yoon, S. J. Myung, J. H. Lee, S. H. Lee, S. M. Lee, S. J. Kim, S. Y. Hwang, H. S. Lee, and C. Y. Kim. 2010. High expression of microRNA-15b predicts a low risk of tumor recurrence following curative resection of hepatocellular carcinoma. *Oncol. Rep.* 23: 113–119.
27. Satzger, I., A. Mattern, U. Kuettler, D. Weinspach, B. Voelker, A. Kapp, and R. Gutzmer. 2010. MicroRNA-15b represents an independent prognostic parameter and is correlated with tumor cell proliferation and apoptosis in malignant melanoma. *Int. J. Cancer* 126: 2553–2562.
28. Cimmino, A., G. A. Calin, M. Fabbri, M. V. Iorio, M. Ferracin, M. Shimizu, S. E. Wojcik, R. I. Aqeilan, S. Zupo, M. Dono, et al. 2005. miR-15 and miR-16 induce apoptosis by targeting BCL2. [Published erratum appears in 2006 *Proc. Natl. Acad. Sci. USA* 103: 2464.] *Proc. Natl. Acad. Sci. USA* 102: 13944–13949.
29. Xia, L., D. Zhang, R. Du, Y. Pan, L. Zhao, S. Sun, L. Hong, J. Liu, and D. Fan. 2008. miR-15b and miR-16 modulate multidrug resistance by targeting BCL2 in human gastric cancer cells. *Int. J. Cancer* 123: 372–379.
30. Dai, X., W. Zhang, H. Zhang, S. Sun, H. Yu, Y. Guo, Z. Kou, G. Zhao, L. Du, S. Jiang, et al. 2014. Modulation of HBV replication by microRNA-15b through targeting hepatocyte nuclear factor 1α. *Nucleic Acids Res.* 42: 6578–6590.
31. Lv, X., H. Jiang, Y. Liu, X. Lei, and J. Jiao. 2014. MicroRNA-15b promotes neurogenesis and inhibits neural progenitor proliferation by directly repressing TET3 during early neocortical development. *EMBO Rep.* 15: 1305–1314.
32. Chen, Z., L. Shao, J. Ye, Y. Li, S. Huang, H. Chen, and S. Cao. 2012. Monoclonal antibodies against NS3 and NS5 proteins of Japanese encephalitis virus. *Hybridoma (Larchmt)* 31: 137–141.
33. Xu, Z., S. B. Xiao, P. Xu, Q. Xie, L. Cao, D. Wang, R. Luo, Y. Zhong, H. C. Chen, and L. R. Fang. 2011. miR-365, a novel negative regulator of interleukin-6 gene expression, is cooperatively regulated by Sp1 and NF-kappaB. *J. Biol. Chem.* 286: 21401–21412.
34. Arimoto, K., H. Takahashi, T. Hishiki, H. Konishi, T. Fujita, and K. Shimotohno. 2007. Negative regulation of the RIG-I signaling by the ubiquitin ligase RNF125. *Proc. Natl. Acad. Sci. USA* 104: 7500–7505.
35. Hwang, S. Y., K. Y. Hur, J. R. Kim, K. H. Cho, S. H. Kim, and J. Y. Yoo. 2013. Biphasic RLR-IFN-β response controls the balance between antiviral immunity and cell damage. *J. Immunol.* 190: 1192–1200.
36. Yoneyama, M., M. Kikuchi, T. Natsukawa, N. Shinobu, T. Imaizumi, M. Miyagishi, K. Taira, S. Akira, and T. Fujita. 2004. The RNA helicase RIG-I has an essential function in double-stranded RNA-induced innate antiviral responses. *Nat. Immunol.* 5: 730–737.
37. Cao, S., Y. Li, J. Ye, X. Yang, L. Chen, X. Liu, and H. Chen. 2011. Japanese encephalitis virus wild strain infection suppresses dendritic cells maturation and function, and causes the expansion of regulatory T cells. *Virol. J.* 8: 39.
38. Ye, J., R. Jiang, M. Cui, B. Zhu, L. Sun, Y. Wang, A. Zohaib, Q. Dong, X. Ruan, Y. Song, et al. 2014. Etanercept reduces neuroinflammation and lethality in mouse model of Japanese encephalitis. *J. Infect. Dis.* 210: 875–889.
39. Mori, Y., T. Okabayashi, T. Yamashita, Z. Zhao, T. Wakita, K. Yasui, F. Hasebe, M. Tadano, E. Konishi, K. Moriishi, and Y. Matsuura. 2005. Nuclear localization of Japanese encephalitis virus core protein enhances viral replication. *J. Virol.* 79: 3448–3458.
40. Wang, H., M. Chiu, Z. Xie, M. Chiu, Z. Liu, P. Chen, S. Liu, J. C. Byrd, N. Muthusamy, R. Garzon, et al. 2012. Synthetic microRNA cassette dosing: pharmacokinetics, tissue distribution and bioactivity. *Mol. Pharm.* 9: 1638–1644.
41. Xu, L. J., Y. B. Ouyang, X. Xiong, C. M. Stary, and R. G. Giffard. 2015. Post-stroke treatment with miR-181 antagomir reduces injury and improves long-term behavioral recovery in mice after focal cerebral ischemia. *Exp. Neurol.* 264: 1–7.
42. Thounaojam, M. C., K. Kundu, D. K. Kaushik, S. Swaroop, A. Mahadevan, S. K. Shankar, and A. Basu. 2014. MicroRNA 155 regulates Japanese encephalitis virus-induced inflammatory response by targeting Src homology 2-containing inositol phosphatase 1. *J. Virol.* 88: 4798–4810.
43. Zhu, B., J. Ye, P. Lu, R. Jiang, X. Yang, Z. F. Fu, H. Chen, and S. Cao. 2012. Induction of antigen-specific immune responses in mice by recombinant baculovirus expressing premembrane and envelope proteins of West Nile virus. *Virol. J.* 9: 132.
44. Dave, R. S., and K. Khalili. 2010. Morphine treatment of human monocyte-derived macrophages induces differential miRNA and protein expression: impact on inflammation and oxidative stress in the central nervous system. *J. Cell. Biochem.* 110: 834–845.

45. Das, S., M. K. Mishra, J. Ghosh, and A. Basu. 2008. Japanese Encephalitis Virus infection induces IL-18 and IL-1beta in microglia and astrocytes: correlation with in vitro cytokine responsiveness of glial cells and subsequent neuronal death. *J. Neuroimmunol.* 195: 60–72.
46. Nazmi, A., K. Dutta, and A. Basu. 2011. RIG-I mediates innate immune response in mouse neurons following Japanese encephalitis virus infection. *PLoS One* 6: e21761.
47. Rehmsmeier, M., P. Steffen, M. Hochsmann, and R. Giegerich. 2004. Fast and effective prediction of microRNA/target duplexes. *RNA* 10: 1507–1517.
48. Krek, A., D. Grün, M. N. Poy, R. Wolf, L. Rosenberg, E. J. Epstein, P. MacMenamin, I. da Piedade, K. C. Gunsalus, M. Stoffel, and N. Rajewsky. 2005. Combinatorial microRNA target predictions. *Nat. Genet.* 37: 495–500.
49. John, B., A. J. Enright, A. Aravin, T. Tuschl, C. Sander, and D. S. Marks. 2004. Human MicroRNA targets. [Published erratum appears in 2005 *PLoS Biol.* 3: e264.] *PLoS Biol.* 2: e363.
50. Oshiumi, H., M. Matsumoto, and T. Seya. 2012. Ubiquitin-mediated modulation of the cytoplasmic viral RNA sensor RIG-I. *J. Biochem.* 151: 5–11.
51. Zohaib, A., X. Duan, B. Zhu, J. Ye, S. Wan, H. Chen, X. Liu, and S. Cao. 2015. The Role of Ubiquitination in Regulation of Innate Immune Signaling. *Curr. Issues Mol. Biol.* 18: 1–10.
52. Chen, C. J., Y. C. Ou, S. Y. Lin, S. L. Raung, S. L. Liao, C. Y. Lai, S. Y. Chen, and J. H. Chen. 2010. Glial activation involvement in neuronal death by Japanese encephalitis virus infection. *J. Gen. Virol.* 91: 1028–1037.
53. Pareek, S., S. Roy, B. Kumari, P. Jain, A. Banerjee, and S. Vrati. 2014. MiR-155 induction in microglial cells suppresses Japanese encephalitis virus replication and negatively modulates innate immune responses. *J. Neuroinflammation* 11: 97.
54. Thounaojam, M. C., D. K. Kaushik, K. Kundu, and A. Basu. 2014. MicroRNA-29b modulates Japanese encephalitis virus-induced microglia activation by targeting tumor necrosis factor alpha-induced protein 3. *J. Neurochem.* 129: 143–154.
55. Nazmi, A., R. Mukhopadhyay, K. Dutta, and A. Basu. 2012. STING mediates neuronal innate immune response following Japanese encephalitis virus infection. *Sci. Rep.* 2: 347.
56. Kato, H., O. Takeuchi, S. Sato, M. Yoneyama, M. Yamamoto, K. Matsui, S. Uematsu, A. Jung, T. Kawai, K. J. Ishii, et al. 2006. Differential roles of MDA5 and RIG-I helicases in the recognition of RNA viruses. *Nature* 441: 101–105.
57. Oshiumi, H., M. Miyashita, N. Inoue, M. Okabe, M. Matsumoto, and T. Seya. 2010. The ubiquitin ligase Riplet is essential for RIG-I-dependent innate immune responses to RNA virus infection. *Cell Host Microbe* 8: 496–509.
58. Kim, M. J., S. Y. Hwang, T. Imaizumi, and J. Y. Yoo. 2008. Negative feedback regulation of RIG-I-mediated antiviral signaling by interferon-induced ISG15 conjugation. *J. Virol.* 82: 1474–1483.
59. Rosenberger, C. M., R. L. Podyminogin, G. Navarro, G. W. Zhao, P. S. Askovich, M. J. Weiss, and A. Aderem. 2012. miR-451 regulates dendritic cell cytokine responses to influenza infection. *J. Immunol.* 189: 5965–5975.
60. Chen, S. T., R. S. Liu, M. F. Wu, Y. L. Lin, S. Y. Chen, D. T. Tan, T. Y. Chou, I. S. Tsai, L. Li, and S. L. Hsieh. 2012. CLEC5A regulates Japanese encephalitis virus-induced neuroinflammation and lethality. *PLoS Pathog.* 8: e1002655.
61. Mishra, M. K., and A. Basu. 2008. Minocycline neuroprotects, reduces microglial activation, inhibits caspase 3 induction, and viral replication following Japanese encephalitis. *J. Neurochem.* 105: 1582–1595.
62. Swarup, V., J. Ghosh, S. Ghosh, A. Saxena, and A. Basu. 2007. Antiviral and anti-inflammatory effects of rosmarinic acid in an experimental murine model of Japanese encephalitis. *Antimicrob. Agents Chemother.* 51: 3367–3370.
63. Das, S., K. Dutta, K. L. Kumawat, A. Ghoshal, D. Adhya, and A. Basu. 2011. Abrogated inflammatory response promotes neurogenesis in a murine model of Japanese encephalitis. *PLoS One* 6: e17225.